

## Heteronuclear NMR Spectroscopy for Lysine NH<sub>3</sub> Groups in Proteins: Unique Effect of Water Exchange on <sup>15</sup>N Transverse Relaxation

Junji Iwahara, Young-Sang Jung, and G. Marius Clore\*

Laboratory of Chemical Physics, National Institute of Diabetes and Digestive and Kidney Disease, National Institutes of Health, Bethesda, Maryland 20892-0520

Received November 21, 2006; E-mail: mariusc@intra.niddk.nih.gov

**Abstract:** In this paper, we present a series of heteronuclear NMR experiments for the direct observation and characterization of lysine NH<sub>3</sub> groups in proteins. In the context of the HoxD9 homeodomain bound specifically to DNA we were able to directly observe three cross-peaks, arising from lysine NH<sub>3</sub> groups, with <sup>15</sup>N chemical shifts around ~33 ppm at pH 5.8 and 35 °C. Measurement of water-exchange rates and various types of <sup>15</sup>N transverse relaxation rates for these NH<sub>3</sub> groups, reveals that rapid water exchange dominates the <sup>15</sup>N relaxation for antiphase coherence with respect to <sup>1</sup>H through scalar relaxation of the second kind. As a consequence of this phenomenon, <sup>15</sup>N line shapes of NH<sub>3</sub> signals in a conventional <sup>1</sup>H–<sup>15</sup>N heteronuclear single quantum coherence (HSQC) correlation experiment are much broader than those of backbone amide groups. A 2D <sup>1</sup>H–<sup>15</sup>N correlation experiment that exclusively observes in-phase <sup>15</sup>N transverse coherence (termed HISQC for heteronuclear in-phase single quantum coherence spectroscopy) is independent of scalar relaxation in the *t*<sub>1</sub> (<sup>15</sup>N) time domain and as a result exhibits strikingly sharper <sup>15</sup>N line shapes and higher intensities for NH<sub>3</sub> cross-peaks than either HSQC or heteronuclear multiple quantum coherence (HMQC) correlation experiments. Coherence transfer through the relatively small *J*-coupling between <sup>15</sup>Nζ and <sup>13</sup>Cε (4.7–5.0 Hz) can be achieved with high efficiency by maintaining in-phase <sup>15</sup>N coherence owing to its slow relaxation. With the use of a suite of triple resonance experiments based on the same design principles as the HISQC, all the NH<sub>3</sub> cross-peaks observed in the HISQC spectrum could be assigned to lysines that directly interact with DNA phosphate groups. Selective observation of functional NH<sub>3</sub> groups is feasible because of hydrogen bonding or salt bridges that protect them from rapid water exchange. Finally, we consider the potential use of lysine NH<sub>3</sub> groups as an alternative probe for larger systems as illustrated by data obtained on the 128-kDa enzyme I dimer.

### Introduction

Lysine side-chain NH<sub>3</sub> groups have a p*K*<sub>a</sub> in the range 9.5–11.0<sup>1–3</sup> and are positively charged at neutral pH. As a result lysine side chains often play an important role in protein function, particularly with regard to protein–protein and protein–nucleic acid recognition, through the formation of salt bridges with carboxylates of glutamate and aspartate and the phosphate groups of DNA and RNA. NMR characterization, however, of lysine NH<sub>3</sub> groups is challenging primarily because of rapid hydrogen exchange with water.<sup>5</sup> NH<sub>3</sub> groups with water-exchange rates greater than ~100 s<sup>-1</sup> are generally undetectable by <sup>1</sup>H NMR. Indeed, Liepinsh and Otting found that the water exchange rate (*k*<sub>ex</sub><sup>water</sup>) for the NH<sub>3</sub> group of free lysine is as fast as 4000 s<sup>-1</sup> at pH 7.0 and 36 °C.<sup>4</sup> Nevertheless, depending on the surrounding environment (e.g., the presence of strong

electrostatic interactions), the exchange rates for some lysine NH<sub>3</sub> groups can be slow enough at lower pH and temperature to permit their observation by <sup>1</sup>H NMR.

In principle one would expect that heteronuclear NMR spectroscopy should be useful for characterizing lysine NH<sub>3</sub> groups.<sup>5</sup> Yet, even when *k*<sub>ex</sub><sup>water</sup> is slow enough to permit their detection by <sup>1</sup>H NMR, cross-peaks corresponding to lysine NH<sub>3</sub> groups are barely visible in a standard <sup>1</sup>H–<sup>15</sup>N heteronuclear single quantum coherence (HSQC) correlation experiment optimized for backbone amides which accounts for why so little is known to date about <sup>15</sup>N NMR of NH<sub>3</sub> groups in proteins. The difficulty in observing <sup>1</sup>H–<sup>15</sup>N correlations for lysine NH<sub>3</sub> groups is due to two factors: (a) the <sup>15</sup>N chemical shift of lysine NH<sub>3</sub> that resonates ~90 ppm upfield from the backbone <sup>15</sup>N resonances and (b) the unique <sup>15</sup>N transverse relaxation properties of NH<sub>3</sub> groups.

In this paper, we demonstrate that <sup>15</sup>N transverse relaxation for lysine NH<sub>3</sub> groups is highly affected by water exchange through scalar relaxation of the second kind.<sup>6,7</sup> Although both NH<sub>3</sub> and CH<sub>3</sub> groups are AX<sub>3</sub> spin-systems, this effect is specific

(1) Brown, L. R.; De Marco, A.; Wagner, G.; Wüthrich, K. *Eur. J. Biochem.* **1976**, *62*, 103–107.

(2) Gao, G.; DeRose, E. F.; Kirby, T. W.; London, R. E. *Biochemistry* **2006**, *45*, 1785–1794.

(3) Gao, G.; Prasad, R.; Lodwig, S. N.; Unkefer, C. J.; Beard, W. A.; Wilson, S. H.; London, R. E. *J. Am. Chem. Soc.* **2006**, *128*, 8104–8105.

(4) Liepinsh, E.; Otting, G. *Magn. Reson. Med.* **1996**, *35*, 30–42.

(5) Farmer, B. T., II; Venters, R. A. *J. Biomol. NMR* **1996**, *7*, 59–71.

(6) Abragam, A. *The Principles of Nuclear Magnetism*; Carendon Press: Oxford, 1961; Chapter VIII, p 309.

to NH<sub>3</sub> groups and constitutes a clear distinction to the case of <sup>13</sup>C transverse relaxation of CH<sub>3</sub> groups. While Kay and co-workers have demonstrated that heteronuclear multiple quantum coherence (HMQC)<sup>8</sup> spectroscopy represents the best experiment for optimal <sup>1</sup>H–<sup>13</sup>C correlation of CH<sub>3</sub> groups,<sup>9,10</sup> we demonstrate that neither HSQC<sup>11</sup> nor HMQC experiments are ideal for NH<sub>3</sub> groups. In both HSQC and HMQC experiments, scalar relaxation via water exchange results in <sup>15</sup>N line shapes for NH<sub>3</sub> groups that are even broader than those of backbone amide groups, even though fast internal motion should result in significantly slower <sup>15</sup>N relaxation for NH<sub>3</sub> groups. To circumvent this problem we have designed an alternative <sup>1</sup>H–<sup>15</sup>N correlation experiment that is completely independent of such scalar relaxation in the <sup>15</sup>N-dimension by forcing the <sup>15</sup>N transverse coherence to always be in-phase with respect to <sup>1</sup>H during the *t*<sub>1</sub>(<sup>15</sup>N) evolution period. This experiment which we refer to as HISQC for heteronuclear in-phase single quantum coherence spectroscopy takes full advantage of the intrinsically slow <sup>15</sup>N relaxation of NH<sub>3</sub> groups, resulting in strikingly better resolution and sensitivity over HMQC and HSQC experiments. We also present a suite of triple resonance experiments based on the same principle for assignment of lysine NH<sub>3</sub> resonances. The application of these methods is illustrated for the 22 kDa HOXD9 homeodomain–DNA complex and the 128 kDa enzyme I dimer.

## Materials and Methods

**NMR Samples.** Samples of the 22-kDa complex between <sup>13</sup>C/<sup>15</sup>N- or <sup>2</sup>H/<sup>15</sup>N-labeled HOXD9 homeodomain and unlabeled 24-bp DNA containing the specific recognition sequence (Shb in ref 12) were prepared as described previously.<sup>12–14</sup> For Figures 1a, 2, and 3a, the sample was dissolved in buffer comprising 10 mM sodium phosphate (pH 5.8) and 93% <sup>1</sup>H<sub>2</sub>O/7% D<sub>2</sub>O and placed in Shigemitsu susceptibility-matched microtubes. To avoid undesired NH<sub>2</sub>D and NHD<sub>2</sub> species, all other data were recorded using a 270-μl solution of 0.6-mM complex in 10 mM sodium phosphate (pH 5.8) and 100% <sup>1</sup>H<sub>2</sub>O sealed in the inner tube of a Shigemitsu external reference coaxial NMR tube (diameters: inner tube, 4.1 mm; outer tube, 5.0 mm). D<sub>2</sub>O for the lock signal was placed in a thin layer between the inner and the outer tube (see later).

Full length <sup>15</sup>N-labeled enzyme I (579 amino acid) from *Thermoanaerobacter tengcongensis* was overexpressed in *E. coli* and purified by affinity- and size-exclusion chromatography. A 270-μl solution of 0.4 mM protein dissolved in 20 mM sodium acetate buffer (pH 5.5), 0.1 mM NaN<sub>3</sub>, 2 mM DTT and 100% <sup>1</sup>H<sub>2</sub>O was sealed in a coaxial tube. Light-scattering data indicated that under these conditions full length enzyme I forms a monodisperse 128-kDa dimer, as reported previously in the literature.<sup>15</sup>

**NMR Spectroscopy.** All NMR experiments except for those reported in Figure 13 were carried out using a Bruker DMX-500 spectrometer equipped with a cryogenic probe (<sup>1</sup>H frequency, 500 MHz). Experiments on the HOXD9 homeodomain–DNA complex were carried out at

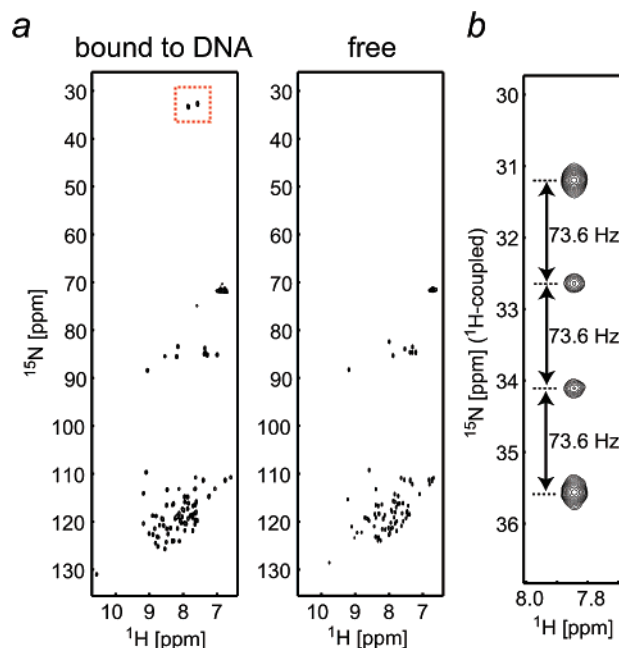


**Figure 1.** <sup>1</sup>H–<sup>15</sup>N HSQC spectra of <sup>13</sup>C/<sup>15</sup>N-labeled HOXD9 homeodomain. (a) 2D <sup>1</sup>H–<sup>15</sup>N HSQC spectra measured at pH 5.8 of the homeodomain bound specifically to a 24-bp DNA duplex (left) and in the free state (right). The spectra were recorded at 35 °C with the <sup>15</sup>N-carrier position at 82 ppm and <sup>15</sup>N rf field strengths of 5.2 kHz for 90° and 180° pulses and 1.2 kHz for composite decoupling during acquisition. <sup>13</sup>C-decoupling was also applied in the <sup>15</sup>N-dimension. The red dashed box indicates the cross-peaks around ~33 ppm that are only observed for the DNA-bound state. (b) Expansion of the F1–<sup>1</sup>H-coupled HSQC spectrum showing the signal at 33.3 ppm enclosed within the dashed box in panel a. The quartet structure indicates that the signals arise from NH<sub>3</sub> groups and the value of <sup>1</sup>J<sub>NH</sub> is 73.6 Hz.

two temperatures (35 and 25 °C). <sup>1</sup>H and <sup>15</sup>N resonances for NH<sub>3</sub> groups were assigned using the suite of triple-resonance experiments shown in Figure 10 along with Lys <sup>1</sup>H/<sup>13</sup>C chemical shifts assigned in our previous studies.<sup>12–14</sup> Spectra on Enzyme I were recorded on a Bruker DRX-800 spectrometer equipped with a cryogenic probe (<sup>1</sup>H frequency, 800 MHz). NMR data were processed using NMRPipe<sup>16</sup> and analyzed with NMRView.<sup>17</sup> Further details of individual NMR experiments are described in the figure captions.

## Results and Discussion

**HSQC Signals from Lysine NH<sub>3</sub> Groups.** The present work was initiated by the observation of cross-peaks with unusual <sup>15</sup>N chemical shifts around 33 ppm observed in the <sup>1</sup>H–<sup>15</sup>N HSQC correlation spectrum of <sup>13</sup>C/<sup>15</sup>N-labeled HOXD9 homeodomain complexed to a 24-bp DNA duplex at pH 5.8 and 35 °C (Figure 1a). The corresponding signals were not observed for the free protein under the same conditions, implying that these signals originate from functional groups involved in DNA-binding. In the F1–<sup>1</sup>H-coupled HSQC spectrum, the cross-peaks at ~33 ppm exhibit a quartet splitting pattern, indicating that they arise from NH<sub>3</sub> groups (Figure 1b). A similar observation has recently been made for glycoside hydrolase.<sup>18</sup> From the

(7) Bax, A.; Ikura, M.; Kay, L. E.; Torchia, D. A.; Tschudin, R. *J. Magn. Reson.* **1990**, *86*, 304–318.

(8) Bax, A.; Griffey, R. H.; Hawkins, B. L. *J. Magn. Reson.* **1983**, *55*, 301–315.

(9) Tugarinov, V.; Hwang, P. M.; Ollerenshaw, J. E.; Kay, L. E. *J. Am. Chem. Soc.* **2003**, *125*, 10420–10428.

(10) Ollerenshaw, J. E.; Tugarinov, V.; Kay, L. E. *Magn. Reson. Chem.* **2003**, *41*, 843–852.

(11) Bodenhausen, G.; Ruben, D. *J. Chem. Phys. Lett.* **1980**, *69*, 185–189.

(12) Iwahara, J.; Zweckstetter, M.; Clore, G. M. *Proc. Natl. Acad. Sci. U.S.A.* **2006**, *103*, 15062–15067.

(13) Iwahara, J.; Clore, G. M. *J. Am. Chem. Soc.* **2006**, *128*, 404–405.

(14) Iwahara, J.; Clore, G. M. *Nature* **2006**, *440*, 1227–1230.

(15) Patel, H. V.; Vyas, K. A.; Savchenko, R.; Roseman, S. *J. Biol. Chem.* **2006**, *281*, 17570–17578.

(16) Delaglio, F.; Grzesiek, S.; Vuister, G. W.; Zhu, G.; Pfeifer, J.; Bax, A. *J. Biomol. NMR* **1995**, *6*, 277–293.

(17) Johnson, B. A.; Blevins, R. A. *J. Biomol. NMR* **1994**, *4*, 603–614.

(18) Poon, D. K. Y.; Schubert, M.; Au, J.; Okon, M.; Withers, S. G.; McIntosh, L. P. *J. Am. Chem. Soc.* **2006**, *128*, 15388–15389.

(19) Tjandra, N.; Grzesiek, S.; Bax, A. *J. Am. Chem. Soc.* **1996**, *118*, 6264–6272.

(20) Permi, P. *J. Biomol. NMR* **2002**, *22*, 27–35.

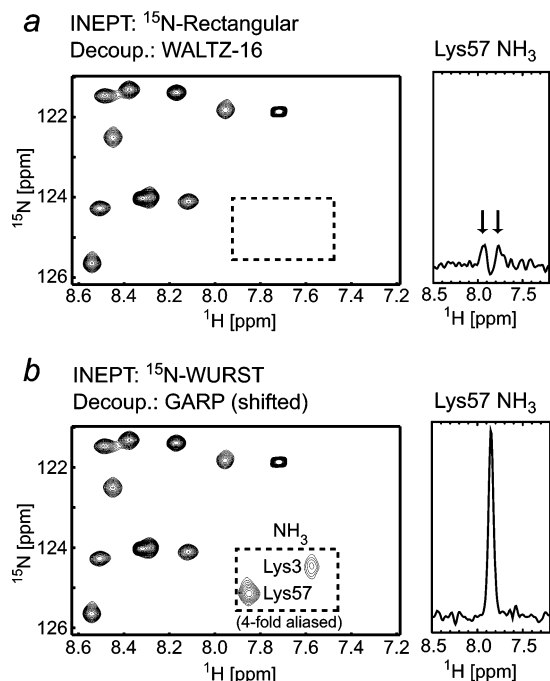


**Figure 2.** Cross-peaks arising from Lys NH<sub>3</sub> groups in the HOXD9 homeodomain–DNA complex are difficult to observe in standard HSQC experiments for backbone amide groups. (a) HSQC spectrum recorded with <sup>15</sup>N rectangular pulses (rf field strength of 5.2 kHz) with the carrier frequency set to 116 ppm. <sup>15</sup>N-WALTZ-16 decoupling ( $\gamma B_1/2\pi = 1.2$  kHz) centered at 116 ppm was applied during acquisition. (b) HSQC spectrum recorded with <sup>15</sup>N WURST inversion pulses (1.25 ms) instead of rectangular 180° pulses. The <sup>15</sup>N carrier frequency was set to 116 ppm for all pulses except the <sup>15</sup>N-GARP ( $\gamma B_1/2\pi = 1.2$  kHz) decoupling sequence during acquisition where the carrier was shifted to 80 ppm to ensure effective decoupling over the complete range of <sup>15</sup>N chemical shifts. All other experimental conditions were the same as those for the spectrum shown in panel a. <sup>13</sup>C-decoupling was applied in the <sup>15</sup>N-dimension. Both spectra were recorded at 35 °C using a Bruker DMX-500 spectrometer at a <sup>1</sup>H-frequency of 500 MHz. The spectral width for the <sup>15</sup>N dimension was 22.9 ppm for each spectrum and the lysine NH<sub>3</sub> cross-peaks are 4-fold aliased. The sample comprised 0.5 mM <sup>13</sup>C/<sup>15</sup>N-labeled HOXD9 homeodomain–DNA complex (pH 5.8). For each panel, a 1D slice along <sup>1</sup>H dimension through the cross-peak of Lys57 NH<sub>3</sub> is also shown (right-hand panels). In the case of the spectrum shown in panel a, the NH<sub>3</sub> cross-peaks are very weak and exhibit doublet splitting (indicated by the arrows).

splitting width of the quartet, the value of the <sup>1</sup>J<sub>NH</sub> scalar coupling for these NH<sub>3</sub> groups was found to be 73.6 Hz, which is considerably smaller than that for backbone amide groups (~93 Hz; ref 19) or glutamine/asparagine side-chain NH<sub>2</sub> groups (~89 Hz; ref 20). The lower shielding and smaller <sup>1</sup>J<sub>NH</sub> coupling for NH<sub>3</sub> groups is in accord with the corresponding observations for CH<sub>3</sub> groups for which the <sup>13</sup>C chemical shift and <sup>1</sup>J<sub>CH</sub> coupling are both considerably smaller than those for planar sp<sup>2</sup> CH groups.<sup>21</sup> The two NH<sub>3</sub> cross-peaks clearly observed in the HSQC experiment were found to originate from Lys3 and Lys57 (see later).

In the standard <sup>1</sup>H–<sup>15</sup>N HSQC experiment used for the observation of protein backbone amide groups with the <sup>15</sup>N carrier position around ~116 ppm, the performance of <sup>15</sup>N 180° pulses and composite decoupling schemes are poor for NH<sub>3</sub> signals around ~33 ppm owing to the limited rf strength employed for <sup>15</sup>N (typically ~5.2 kHz for hard pulses; ~1.2 kHz for decoupling), as we found previously for the arginine

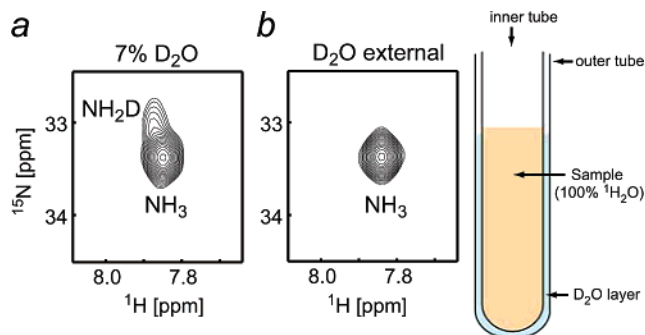


**Figure 3.** Cross-peak of Lys57 NH<sub>3</sub> in the <sup>13</sup>C/<sup>15</sup>N-HOXD9 homeodomain–DNA complex observed in the HSQC spectrum recorded on samples dissolved in (a) 93% <sup>1</sup>H<sub>2</sub>O and 7% D<sub>2</sub>O and (b) 100% <sup>1</sup>H<sub>2</sub>O. The shoulder of the cross-peak in panel a corresponds to the NH<sub>2</sub>D species. In panel b the NMR sample is placed in the inner tube of a coaxial system while D<sub>2</sub>O for the NMR lock is located in the external layer between the outer and the inner tubes. The shoulder observed in the cross-peak in panel a is no longer present in the cross-peak in panel b.

side-chain <sup>15</sup>Nε.<sup>22</sup> The problem is more severe for NH<sub>3</sub> cross-peaks because of the larger offset (~4.2 kHz at 500 MHz spectrometer). On a 500 MHz spectrometer, application of a rectangular <sup>15</sup>N 180° pulse at 116 ppm with an rf field strength of  $\gamma B_1/2\pi = 5.2$  kHz to a magnetization  $M_0$  at 33 ppm along +z results in  $M_z = +0.019M_0$  as opposed to  $-M_0$ . With two INEPT schemes, the signal at 33 ppm is reduced to 24% of the maximum owing to imperfections of the rectangular <sup>15</sup>N 180 pulses. The corresponding values at 600 and 800 MHz are 12% and 1%, respectively. In addition, <sup>15</sup>N-WALTZ decoupling<sup>23</sup> at 116 ppm with  $\gamma B_1/2\pi = 1.2$  kHz does not reach 33 ppm even at 500 MHz resulting in doublet splitting and further reduction of the signal intensity. (Note the effective range of the WALTZ-16 decoupling scheme is  $\pm 1.2\gamma B_1/2\pi$  in Hz.) Figure 2a shows the NH<sub>3</sub> region of an HSQC spectrum recorded at 500 MHz with the <sup>15</sup>N carrier position at 116 ppm with rf field strengths of 5.2 kHz for hard <sup>15</sup>N pulses and 1.2 kHz for decoupling. As expected from the above considerations, the NH<sub>3</sub> cross-peaks are indeed very weak in this spectrum and doublet splitting in the <sup>1</sup>H dimension is observed. Thus, detection of NH<sub>3</sub> cross-peaks is difficult with a standard HSQC experiment optimized for backbone amide groups at high magnetic field, even if the water-exchange rates are slow enough to permit the observation of NH<sub>3</sub> resonances by <sup>1</sup>H NMR.

Figure 2b shows the HSQC spectrum recorded with broadband <sup>15</sup>N WURST-20 inversion pulses<sup>24</sup> for the INEPT transfers, and <sup>15</sup>N-GARP<sup>25</sup> centered at 82 ppm for simultaneous decoupling of <sup>15</sup>NH, <sup>15</sup>NH<sub>2</sub>, and <sup>15</sup>NH<sub>3</sub>. In this HSQC spectrum, the NH<sub>3</sub> cross-peaks are singlets with much higher intensities, while backbone NH cross-peaks are unperturbed relative to a standard HSQC spectrum.

Two features should be noted regarding the NH<sub>3</sub> cross-peaks observed in the HSQC spectrum shown Figure 2b. First, the cross-peaks appear to be asymmetric with broad shoulders located at the upper portion of the NH<sub>3</sub> cross-peaks (Figure 3a). These shoulders correspond to the signals of NH<sub>2</sub>D which disappear upon use of a coaxial NMR tube, in which D<sub>2</sub>O for the NMR lock signal is placed in a thin outer layer and the

(22) Iwahara, J.; Clore, G. M. *J. Biomol. NMR* **2006**, *36*, 251–257.

(23) Shaka, A. J.; Keeler, J.; Freeman, R. *J. Magn. Reson.* **1983**, *52*, 313–340.

(24) Kupce, E.; Freeman, R. *J. Magn. Reson.* **1995**, *127*, 36–48.

(25) Shaka, A. J.; Keeler, J. *Prog. NMR Spectrosc.* **1987**, *19*, 47–129.

(21) Zwahlen, C.; Legault, P.; Vincent, S. J. F.; Greenblatt, J.; Konrat, R.; Kay, L. E. *J. Am. Chem. Soc.* **1997**, *119*, 6711–6721.

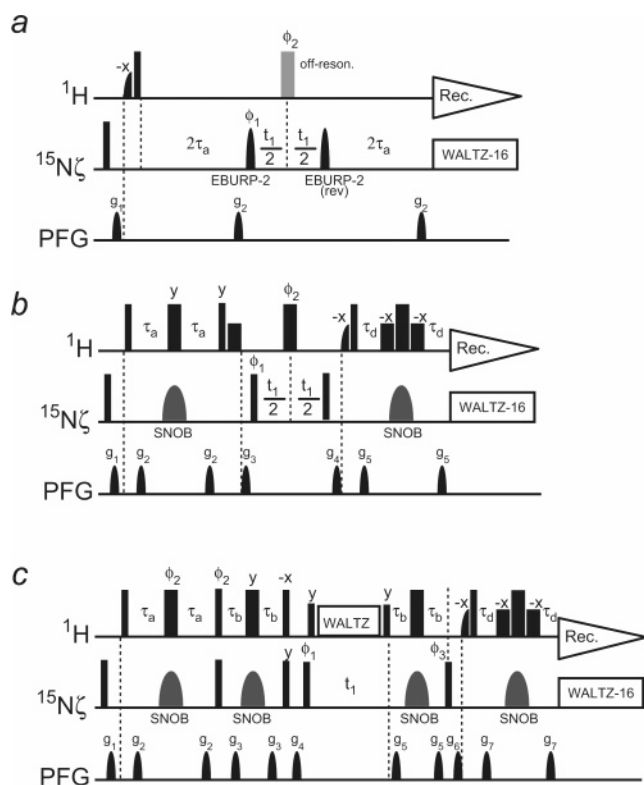


**Figure 4.** 2D  $^1\text{H}$ – $^{15}\text{N}$  correlation experiments for the detection of Lys  $^{15}\text{NH}_3$  groups: (a) HMQC, (b) HSQC, and (c) HISQC. Thin and thick bars represent  $90^\circ$  and  $180^\circ$  pulses, respectively. Water-selective half-Gaussian (2.0 ms) and soft-rectangular (1.4 ms) pulses are represented by half-bell and short bold shapes, respectively. A gray bell shape for  $^{15}\text{N}$  represents a  $r$ -SNOB  $180^\circ$  pulse<sup>29</sup> (1.03 ms) for inversion and refocusing. Unless indicated otherwise, pulse phases are along  $x$ . For all pulse sequences, the  $^1\text{H}$  carrier position was set at the water resonance and the  $^{15}\text{N}$  carrier position at 33 ppm. Rectangular  $^{15}\text{N}$   $90^\circ$  pulses were applied with  $\gamma B_1/2\pi = 2.6$  kHz. The delay  $\tau_a$  was optimized at 2.7 ms, which is considerably shorter than  $(4^1J_{\text{NH}})^{-1}$  ( $=3.4$  ms) because of the relatively fast  $^1\text{H}$  relaxation for  $\text{NH}_3$  groups. Quadrature detection in the  $t_1$  domain was achieved using States-TPPI, incrementing the phase  $\phi_1$ . Field-gradients were optimized to minimize the water signal. (a) The water flip-back HMQC experiment. The gray bar represents an off-resonance  $^1\text{H}$  rectangular  $180^\circ$  pulse that does not affect water. EBURP-2 pulses<sup>28</sup> (1.6 ms) were applied as  $^{15}\text{N}$  $\zeta$ -selective  $90^\circ$  pulses (the second one is time-reversal). Phase cycles:  $\phi_1 = \{x, -x\}$ ;  $\phi_2 = \{2x, 2y, 2(-x), 2(-y)\}$ ; rec. =  $\{x, 2(-x), x\}$ . (b) The water flip-back HSQC experiment. The delay  $\tau_d$  is  $\tau_a$  minus the length of water-selective rectangular  $90^\circ$  pulse. Phase cycles:  $\phi_1 = \{x, -x\}$ ;  $\phi_2 = \{2x, 2(-x)\}$ ; rec. =  $\{x, -x\}$ . (c) The water flip-back HISQC experiment. The delay  $\tau_b$  is set to 1.3 ms. To maintain  $^{15}\text{N}$  in-phase magnetization,  $^1\text{H}$  WALTZ-16 decoupling ( $\gamma B_1/2\pi = 3.3$  kHz) is applied along  $x$  during  $t_1$  in a synchronized mode, sandwiched by additional  $^1\text{H}$   $90^\circ$  pulses along  $y$  to minimize saturation and dephasing of water magnetization.<sup>27</sup> Phase cycles:  $\phi_1 = \{y, -y\}$ ;  $\phi_2 = \{2(y), 2(-y)\}$ ;  $\phi_3 = \{4x, 4(-x)\}$ ; rec. =  $\{x, 2(-x), x, -x, 2x, -x\}$ . The third  $^1\text{H}$   $90^\circ$  pulse along  $-x$  (before the gradient  $g_4$ ) serves two purposes: it purges unnecessary  $^{15}\text{N}$  antiphase magnetization by generating multiple quantum coherence and it flips the water magnetization back to  $+z$ .

inner tube contains the NMR sample without  $\text{D}_2\text{O}$  to avoid the presence of  $\text{NH}_2\text{D}$  and  $\text{NHD}_2$  species (Figure 3b). We therefore used coaxial samples for all subsequent NMR experiments for  $\text{NH}_3$  groups. Second, the  $^{15}\text{N}$  line widths for the  $\text{NH}_3$  cross-peaks in the HSQC spectrum shown in Figure 2b appear broader than those for the backbone NH cross-peaks, although the intrinsic  $^{15}\text{N}$  relaxation for an  $\text{NH}_3$  group should be much slower than that for an NH group owing to fast rotation about the  $\text{N}\zeta\text{—C}\epsilon$  bond. In the following sections, we will address the underlying basis for this observation.

**$\text{NH}_3$  Cross-Peaks Exhibit Strikingly Sharper  $^{15}\text{N}$  Line Shapes in the HISQC Experiment.** We designed three 2-D  $^1\text{H}$ – $^{15}\text{N}$  heteronuclear correlation experiments for the selective observation of  $\text{NH}_3$  groups: namely, HMQC, HSQC and HISQC (Figure 4, parts a, b, and c, respectively). Since water exchange is rapid for  $\text{NH}_3$  groups, each experiment implements a water flip-back scheme<sup>26,27</sup> for better sensitivity. Although the HISQC experiment is a derivative of the “decoupled HSQC” proposed by Bax and co-workers,<sup>7</sup> this terminology is not adopted here to avoid confusion. In the HISQC pulse sequence,  $^{15}\text{N}$  transverse magnetization during  $t_1$  evolution is forced to always be in-phase ( $N_x$  or  $N_y$ ) with respect to  $^1\text{H}$  with continuous use of WALTZ-16  $^1\text{H}$ -decoupling rather than a single  $180^\circ$  pulse. Compared to the HSQC experiment, a  $\text{NH}_3$  signal in the HISQC experiment should be scaled down by an additional factor of  $3 \cos^4 2\pi^1J_{\text{NH}}\tau_b \sin^2 2\pi^1J_{\text{NH}}\tau_b$  owing to schemes for coherence transfers between  $2N_y\text{H}_z$  and  $N_x$ . The scaling factor is maximized to be 0.44 by setting  $\tau_b = 1.3$  ms for  $^1J_{\text{NH}} = 74$  Hz. All three experiments use  $^{15}\text{N}$  shaped pulses (EBURP-2  $90^\circ$  pulse<sup>28</sup> for the HMQC; and  $r$ -SNOB  $180^\circ$  pulses<sup>29</sup> for the HSQC and HISQC) for selective observation of the  $^{15}\text{N}$  signals around 33 ppm.

The spectra recorded with the above three experiments exhibited striking differences. Figure 5 shows  $\text{NH}_3$ -selective (a) HMQC, (b) HSQC, and (c) HISQC spectra recorded at  $35^\circ\text{C}$  on the  $^2\text{H}/^{15}\text{N}$ -labeled HOXD9 homeodomain–DNA complex. All three spectra were recorded with the same number of scans and  $t_1$  time points (140 complex points;  $t_1^{\text{max}} = 168$  ms) and processed identically. Peak heights in the HSQC and HMQC spectra are almost identical, but the signals are broader in the HMQC, because of the additional exchange broadening of  $^1\text{H}$  transverse magnetization during the  $t_1$  evolution period of the HMQC. (Note that the effect of passive coupling for protons should be negligible because of the use of  $^2\text{H}/^{15}\text{N}$ -labeled protein.) Of the three spectra, the HISQC exhibits the highest intensity signals. This may at first appear surprising given that the HISQC experiment suffers from the additional loss of sensitivity as noted above. Further, the line widths in the HISQC spectrum are by far the narrowest of the three spectra. Although the  $\text{NH}_3$  signal arising from Lys55 is barely discernible as a small shoulder of the Lys3 cross-peak in the HSQC and HMQC spectra, it is clearly observed as an isolated cross-peak in the HISQC spectrum. This dramatic result suggests that  $^{15}\text{N}$  transverse relaxation during  $t_1$  in the HISQC experiment is much slower than that for the HSQC experiment.

**Effect of Water Exchange on  $^{15}\text{N}$  Transverse Relaxation of the  $\text{NH}_3$  Group.** To explain the striking difference between the HISQC and HSQC spectra shown in Figure 5, we first discuss various theoretical aspects of  $^{15}\text{N}$  relaxation of  $\text{NH}_3$  groups. While little is known about the  $^{15}\text{N}$  relaxation properties of the  $\text{NH}_3$  group, the theory of  $^{13}\text{C}$  relaxation for  $\text{CH}_3$  groups in macromolecules is well established.<sup>30–34</sup> Considering that

(26) Grzesiek, S.; Bax, A. *J. Am. Chem. Soc.* **1993**, *115*, 12593–12594.

(27) Kay, L. E.; Xu, G. Y.; Yamazaki, T. *J. Magn. Reson., Ser. A* **1994**, *109*, 129–133.

(28) Geen, H.; Freeman, R. *J. Magn. Reson.* **1991**, *93*, 93–141.

(29) Kupce, E.; Boyd, J.; Campbell, I. D. *J. Magn. Reson., Ser. B* **1995**, *106*, 300–303.

(30) Kay, L. E.; Bull, T. E.; Nicholson, L. K.; Griesinger, C.; Schwalbe, H.; Bax, A.; Torchia, D. A. *J. Magn. Reson.* **1992**, *100*, 538–558.

both NH<sub>3</sub> and CH<sub>3</sub> are AX<sub>3</sub> spin systems and that <sup>15</sup>N chemical shift anisotropy (CSA) for lysine NH<sub>3</sub> measured by solid-state NMR is as small as 15 ppm,<sup>35</sup> it is likely that many aspects of the theory of <sup>13</sup>C relaxation of CH<sub>3</sub> groups is applicable to the <sup>15</sup>N relaxation of lysine NH<sub>3</sub> groups in proteins.

By analogy with the theory of <sup>13</sup>C relaxation for CH<sub>3</sub> groups, the <sup>15</sup>N transverse relaxation processes for the inner and outer components of the quartet decay as single exponentials with rates  $R_2^{\text{in}}$  and  $R_2^{\text{out}}$ , respectively, where  $R_2^{\text{in}} < R_2^{\text{out}}$ , as a consequence of cross-correlation between three <sup>15</sup>N-<sup>1</sup>H dipole-dipole (DD) interactions. In contrast to CSA-DD cross-correlation, <sup>15</sup>N-<sup>1</sup>H DD cross-correlation cannot be cancelled out by a <sup>1</sup>H 180° pulse, because this simply swaps two equivalent components (i.e., inner ↔ inner; outer ↔ outer). Under conditions where the spectral density function at zero frequency is dominant, the transverse relaxation rates are given by<sup>10</sup>

$$R_2^{\text{in}} = R_2^{\text{slow}} + \frac{3}{2} R_{\text{sc}} \quad (1)$$

$$R_2^{\text{out}} = R_2^{\text{fast}} + \frac{3}{2} R_{\text{sc}} \quad (2)$$

$$R_2^{\text{slow}} = \frac{1}{45} \left( \frac{\mu_0}{4\pi} \right)^2 S_{\text{axis}}^2 \gamma_{\text{H}}^2 \gamma_{\text{N}}^2 \hbar^2 \frac{1}{r_{\text{NH}}^6} \tau_r \quad (3)$$

$$R_2^{\text{fast}} = 9R_2^{\text{slow}} = \frac{1}{5} \left( \frac{\mu_0}{4\pi} \right)^2 S_{\text{axis}}^2 \gamma_{\text{H}}^2 \gamma_{\text{N}}^2 \hbar^2 \frac{1}{r_{\text{NH}}^6} \tau_r \quad (4)$$

where  $R_2^{\text{slow}}$  and  $R_2^{\text{fast}}$  are the intrinsic <sup>15</sup>N relaxation rates for the inner and outer components;  $R_{\text{sc}}$  is the rate for scalar relaxation of the second kind<sup>6,7</sup> arising from one <sup>1</sup>H nucleus of the NH<sub>3</sub> group (the coefficient of  $3/2$  in front of  $R_{\text{sc}}$  in eqs 1 and 2 arises from an average over contributions from coherence terms such as  $N_x$ ,  $2N_yH_z$ ,  $4N_xH_zH_z$ , and  $8N_yH_zH_zH_z$  that interconvert rapidly because of  $^1J_{\text{NH}}$  evolution);  $S_{\text{axis}}^2$  is a generalized order parameter<sup>36</sup> for the symmetry axis of the NH<sub>3</sub> group; and  $\tau_r$  is the rotational correlation time of the macromolecule. In the case of the HOXD9 homeodomain-DNA complex,  $\tau_r$  was determined to be 11.7 ns at 35 °C from analysis of backbone <sup>15</sup>N relaxation data, which predicts values of  $R_2^{\text{slow}} = 0.94 \text{ s}^{-1}$  and  $R_2^{\text{fast}} = 8.5 \text{ s}^{-1}$  for an NH<sub>3</sub> group with  $S_{\text{axis}}^2 = 0.8$ .

The scalar relaxation term  $R_{\text{sc}}$  arises from autorelaxation of longitudinal magnetization of the coupled <sup>1</sup>H nucleus through mechanisms other than interactions within the spin-system. In the case of a CH<sub>3</sub> group, the sole source of  $R_{\text{sc}}$  is considered to be <sup>1</sup>H-<sup>1</sup>H DD interactions with external <sup>1</sup>H nuclei. The biggest difference between CH<sub>3</sub> and NH<sub>3</sub> spin systems is the presence of water exchange for the NH<sub>3</sub> group. Just as Grzesiek and Bax<sup>37</sup> considered for the case of a  $2N_zH_z$  term for a NH system,  $R_{\text{sc}}$

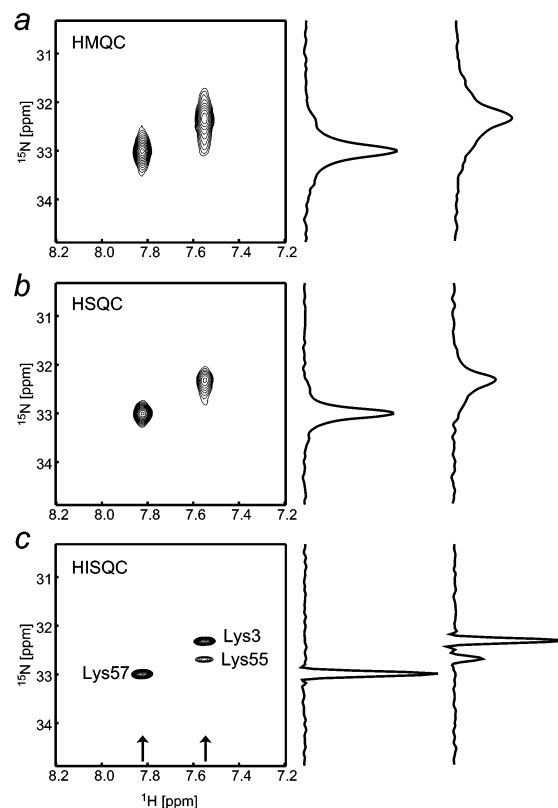


**Figure 5.** 2D <sup>1</sup>H-<sup>15</sup>N correlation spectra recorded at 35 °C on the <sup>2</sup>H/<sup>15</sup>N-HOXD9 homeodomain-DNA complex (pH 5.8) using the pulse sequences shown in Figure 4: (a) HMQC, (b) HSQC, and (c) HISQC. For each spectrum, the <sup>15</sup>N-dimension was acquired with 140 complex points ( $t_1^{\text{max}} = 168 \text{ ms}$ ) and 8 scans per FID were accumulated. Data were processed identically, applying a 30°-shifted squared cosine-bell window function followed by zero-filling to 512 points for the <sup>15</sup>N dimension. F1-slices at the positions indicated by the arrows are shown. Contour levels and scaling of the slices are identical for all panels.

for a NH<sub>3</sub> group should include the contribution from water exchange and be given by

$$R_{\text{sc}} = \rho_{\text{HH}} + k_{\text{ex}}^{\text{water}} \quad (5)$$

where  $\rho_{\text{HH}}$  represents the rate for DD interactions with external <sup>1</sup>H nuclei and  $k_{\text{ex}}^{\text{water}}$  is the water-exchange rate.

To experimentally investigate the properties of <sup>15</sup>N transverse relaxation for NH<sub>3</sub> groups and the contribution of scalar relaxation, we analyzed the line shapes of the NH<sub>3</sub> quartet in F1-<sup>1</sup>H-coupled HSQC spectra measured at 35 and 25 °C on the <sup>2</sup>H/<sup>15</sup>N-HOXD9 homeodomain-DNA complex (Figure 6). The <sup>15</sup>N-slices (black) are taken from spectra processed with no window function in the <sup>15</sup>N dimension. The NH<sub>3</sub> cross-peak of Lys57 is the only NH<sub>3</sub> cross-peak that exhibits an isolated analyzable quartet (see Figure 5). In the F1-<sup>1</sup>H-coupled HSQC experiment, not only the  $2N_yH_z^a \rightarrow 2N_yH_z^b$  process but also the  $2N_yH_z^a \rightarrow 2N_yH_z^c$  and  $2N_yH_z^b \rightarrow 2N_yH_z^c$  coherence transfers occurring during the  $t_1$ -evolution period generate observable

(31) Nicholson, L. K.; Kay, L. E.; Baldisseri, D. M.; Arango, J.; Young, E. P.; Bax, A.; Torchia, A. *Biochemistry* **1992**, *31*, 5253–5263.  
 (32) Werbelow, L. G.; Grant, D. M. *J. Chem. Phys.* **1975**, *63*, 4742–4749.  
 (33) Kay, L. E.; Torchia, D. A. *J. Magn. Reson.* **1991**, *95*, 536–547.

(34) Palmer, A. G.; Hochstrasser, R. A.; Millar, D. P.; Rance, M.; Wright, P. E. *J. Am. Chem. Soc.* **1993**, *115*, 6333–6345.  
 (35) Sarkar, S. K.; Hiyama, Y.; Niu, C. H.; Young, P. E.; Gerig, P. E.; Gerig, J. T.; Torchia, D. A. *Biochemistry* **1987**, *26*, 6793–6800.  
 (36) Lipari, G.; Szabo, A. *J. Am. Chem. Soc.* **1982**, *104*, 4546–4559.  
 (37) Grzesiek, S.; Bax, A. *J. Biomol. NMR* **1993**, *3*, 627–638.

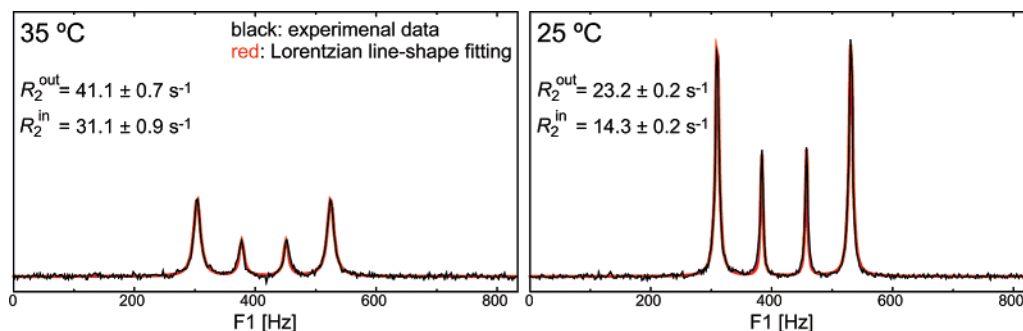


**Figure 6.** Lorentzian line shape fitting of F1 slices taken from the F1-<sup>1</sup>H-coupled HSQC spectra recorded on the <sup>2</sup>H/<sup>15</sup>N-HOXD9 homeodomain–DNA complex (pH 5.8). The experimental data for Lys57 NH<sub>3</sub> at 35 °C (left) and 25 °C (right) are shown in black. The red lines represent the best fit traces obtained by nonlinear least-squares Lorentzian line shape fitting against the experimental data, using eq 7. The pulse sequence used to record the spectra was similar to that shown in Figure 4b, but lacks the <sup>1</sup>H 180° pulse in the middle of *t*<sub>1</sub>-evolution period and the phase of the initial water-selective 90° pulse was changed to  $-x$  for water flip-back. Experimental data were recorded with *t*<sub>1</sub><sup>max</sup> = 269 ms and no window function was applied to the <sup>15</sup>N-dimension in data processing. Relaxation rates for the inner and outer components of the <sup>15</sup>N quartet derived from the fitting procedure are also shown.

**Table 1.** Summary of <sup>15</sup>N Transverse Relaxation and Water-Exchange Rates for the NH<sub>3</sub> Group of Lys57<sup>a</sup>

rates (s <sup>-1</sup> )	35 °C	25 °C
$R_2^{\text{in}b}$	31.1 ± 0.9	14.3 ± 0.2
$R_2^{\text{out}b}$	41.1 ± 0.7	23.2 ± 0.2
$R_2^{\text{slow}c}$	1.3 ± 0.1	1.1 ± 0.1
$R_2^{\text{fast}c}$	11.4 ± 1.2	10.0 ± 0.3
$R_{\text{sc}}^c$	19.9 ± 0.7	8.8 ± 0.2
$k_{\text{ex}}^{\text{water}d}$	18.7 ± 0.3	6.9 ± 0.3
$0.25R_2^{\text{fast}} + 0.75R_2^{\text{slow}e}$	3.8 ± 0.3	3.3 ± 0.1
$R_2^{\text{app}}(N_i)^f$	4.5 ± 0.2	4.4 ± 0.1

<sup>a</sup> Symbols are as defined in eqs 1–5. <sup>b</sup> From Lorentzian line shape fitting against the quartet in the F1-<sup>1</sup>H-coupled HSQC. <sup>c</sup> From  $R_2^{\text{in}}$  and  $R_2^{\text{out}}$  with the constraint that  $R_2^{\text{fast}} = 9R_2^{\text{slow}}$ . <sup>d</sup> From CLEANEX-HISQC experiment. <sup>e</sup> Corresponds to the initial rate for the in-phase term (no scalar relaxation).<sup>33</sup> <sup>f</sup> From relaxation measurements shown in Figure 8.

magnetization. Thus, modulation of the antiphase <sup>15</sup>N term by  $^1J_{\text{NH}}$  and chemical shift evolution is given by

$$(\cos^3 \pi^1 J_{\text{NH}} t_1 - 2 \sin^2 \pi^1 J_{\text{NH}} t_1 \cos \pi^1 J_{\text{NH}} t_1) \cos \Omega t_1 = \frac{3}{8} \cos(\Omega - 3\pi^1 J_{\text{NH}}) t_1 + \frac{1}{8} \cos(\Omega - \pi^1 J_{\text{NH}}) t_1 + \frac{1}{8} \cos(\Omega + \pi^1 J_{\text{NH}}) t_1 + \frac{3}{8} \cos(\Omega + 3\pi^1 J_{\text{NH}}) t_1 \quad (6)$$

resulting in a 3:1:1:3 quartet structure providing the relaxation properties of each component of the quartet are the same. Assuming that the inner and outer components of the quartet decay in a single-exponential manner with rate constants  $R_2^{\text{out}}$  and  $R_2^{\text{in}}$ , respectively, the line shape of the quartet is given by

$$A(\nu) = \frac{3aR_2^{\text{out}}}{R_2^{\text{out}^2} + 4\pi^2(\nu_0 - \nu)^2} + \frac{aR_2^{\text{in}}}{R_2^{\text{in}^2} + 4\pi^2(\nu_0 + ^1J_{\text{NH}} - \nu)^2} + \frac{aR_2^{\text{in}}}{R_2^{\text{in}^2} + 4\pi^2(\nu_0 + 2^1J_{\text{NH}} - \nu)^2} + \frac{3aR_2^{\text{out}}}{R_2^{\text{out}^2} + 4\pi^2(\nu_0 + 3^1J_{\text{NH}} - \nu)^2} \quad (7)$$

where  $\nu$  is the frequency in Hz,  $\nu_0$  is the peak position of the lowest frequency component, and  $a$  is a scaling factor. The red lines in Figure 6 were obtained by nonlinear least-squares fitting, optimizing the five parameters in eq 7:  $R_2^{\text{in}}$ ,  $R_2^{\text{out}}$ ,  $a$ ,  $\nu_0$ , and  $^1J_{\text{NH}}$ . The calculated curves are in excellent agreement with the

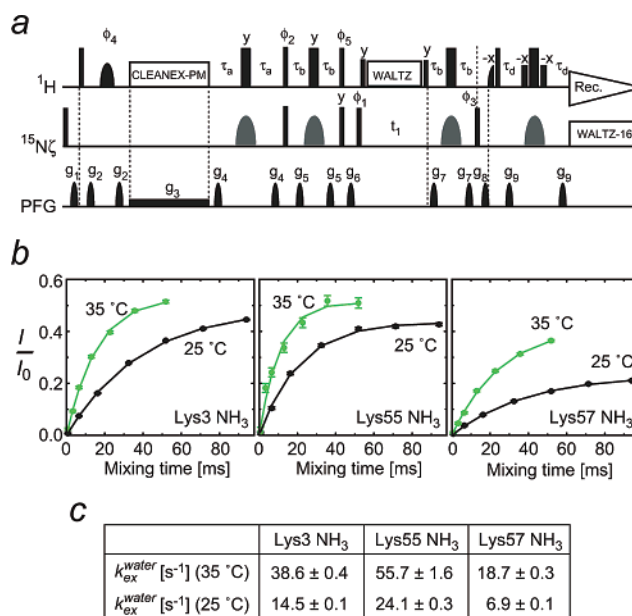


**Figure 7.** Measurement of water exchange rates for Lys NH<sub>3</sub> groups. (a) CLEANEX-HISQC pulse sequence to measure water exchange rates for Lys NH<sub>3</sub> groups. The CLEANEX component was implemented as described previously.<sup>38,39</sup> Phase cycles:  $\phi_1 = \{y, -y\}$ ;  $\phi_2 = y$ ;  $\phi_3 = \{4x, 4(-x)\}$ ;  $\phi_4 = \{2y, 2x\}$ ;  $\phi_5 = \{2(-x), 2x\}$ ; rec. =  $\{x, 2(-x), x, -x, 2x, -x\}$ . The other experimental conditions are the same as those for Figure 4c. (b) Buildup curves for signals arising from exchange between water and lysine NH<sub>3</sub> at 35 °C (green) and 25 °C (black). Seven time-points were used for each measurement. The vertical axis represents the ratio of  $I$  to  $I_0$ , where  $I$  is the signal intensity observed in the CLEANEX-HISQC and  $I_0$  is that in the reference HSQC (Figure 4c). (c) Values of  $k_{\text{ex}}^{\text{water}}$  exchange rates at 35 and 25 °C.

experimental data, indicating that the individual components of the quartet do indeed decay in a single-exponential manner resulting in Lorentzian line shapes. The values of the relaxation rates obtained in this manner are as follows:  $R_2^{\text{out}} = 41.1 \pm 0.7$  s<sup>-1</sup> and  $R_2^{\text{in}} = 31.1 \pm 0.9$  s<sup>-1</sup> at 35 °C;  $R_2^{\text{out}} = 23.2 \pm 0.2$  s<sup>-1</sup> and  $R_2^{\text{in}} = 14.1 \pm 0.2$  s<sup>-1</sup> at 25 °C. It should be noted that the relaxation rates at 25 °C are significantly slower than those at 35 °C, although one might expect the opposite result owing to the increased  $\tau_r$  at the lower temperature. Assuming that the relationship  $R_2^{\text{fast}} = 9R_2^{\text{slow}}$  is valid, we obtain values of  $R_2^{\text{slow}}$ ,  $R_2^{\text{fast}}$  and  $R_{\text{sc}}$  from the experimental  $R_2^{\text{in}}$  and  $R_2^{\text{out}}$  rates using eqs 1 and 2, as shown in Table 1.

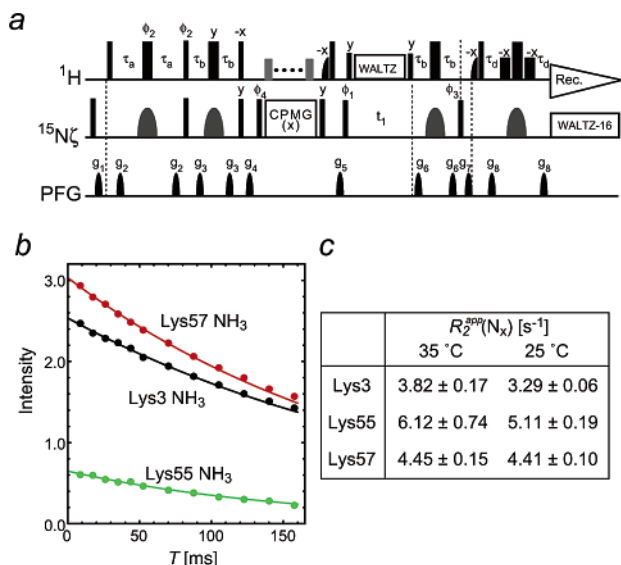


**Figure 8.** <sup>15</sup>N transverse relaxation for the in-phase  $N_x$  term. (a) Pulse sequence used to measure <sup>15</sup>N  $R_2$  rates for  $N_x$  of NH<sub>3</sub>. For the CPMG pulse train, rectangular <sup>15</sup>N 180° pulses were applied along  $x$  with  $\gamma B_1/2\pi = 2.6$  kHz. Although not essential for NH<sub>3</sub> because of small CSA, a semiselective <sup>1</sup>H 180° pulse that does not affect the water magnetization was applied once every 4 ms during the CPMG scheme to suppress CSA-DD cross-correlations. Phase cycles:  $\phi_4 = \{8y, 8(-y)\}$ , rec. =  $\{x, 2(-x), x, -x, 2x, -x, -x, 2x, -x, x, 2(-x), x\}$ . The other experimental conditions are the same as those in Figure 4c. As Kay et al. pointed out for the case of a CH<sub>3</sub> group,<sup>30</sup> the apparent  $R_2$  rates for  $N_x$  of a NH<sub>3</sub> group will be affected by the delay  $\tau_b$ , since  $a_{\text{in}}$  and  $a_{\text{out}}$  in eq 8 depend on  $\tau_b$ . Here, the delay  $\tau_b$  was set to the same value as that used in the HISQC pulse sequence shown in Figure 4c, since our purpose was to investigate <sup>15</sup>N transverse relaxation properties in the context of the HISQC experiment. (b) <sup>15</sup>N transverse relaxation decay for  $N_x$  observed at 35 °C. The measurements were carried out using the <sup>2</sup>H/<sup>15</sup>N-labeled HOXD9 homeodomain–DNA complex (pH 5.8). (c) Apparent <sup>15</sup>N  $R_2$  rates for lysine NH<sub>3</sub> groups obtained at 35 °C and 25 °C. Since <sup>15</sup>N transverse relaxation for a NH<sub>3</sub> group is expected to be biexponential, the values obtained are meaningful only in a phenomenological sense (see main text). These values are determined using single-exponential fitting against the initial (first 72 ms) portion of the experimental decays, and the curves depicted as solid lines in part b are those calculated from this fitting procedure.

From the above analysis, the scalar relaxation rate  $R_{\text{sc}}$  was found to be highly sensitive to temperature ( $19.9 \pm 0.7$  s<sup>-1</sup> at 35 °C versus  $8.8 \pm 0.15$  s<sup>-1</sup> at 25 °C), whereas  $R_2^{\text{slow}}$  and  $R_2^{\text{fast}}$  were insensitive. The temperature-dependence of  $R_2^{\text{in}}$  (or  $R_2^{\text{out}}$ ) is primarily due to that of  $R_{\text{sc}}$ . Further, the contribution of the scalar relaxation term ( $1.5R_{\text{sc}}$ ) to  $R_2^{\text{in}}$  and  $R_2^{\text{out}}$  is very large: 96% and 73%, respectively, at 35 °C (92% and 57%, respectively, at 25 °C). Thus,  $R_2^{\text{in}}$  and  $R_2^{\text{out}}$  are dominated by scalar relaxation.

Given the temperature-dependence of  $R_{\text{sc}}$ , it is likely that the water-exchange rate  $k_{\text{ex}}^{\text{water}}$  in eq 5 contributes significantly to  $R_{\text{sc}}$ , particularly in the present case of a deuterated protein for which  $\rho_{\text{HH}}$  is small ( $< 1$  s<sup>-1</sup>).<sup>9</sup> We analyzed water-exchange rates for lysine NH<sub>3</sub> groups using the pulse sequence shown in Figure 7. This experiment makes use of the CLEANEX-PM scheme<sup>38,39</sup> followed by the HISQC sequence. The values of the  $k_{\text{ex}}^{\text{water}}$  rates were calculated from the buildup curves (Figure 7b,c). For the

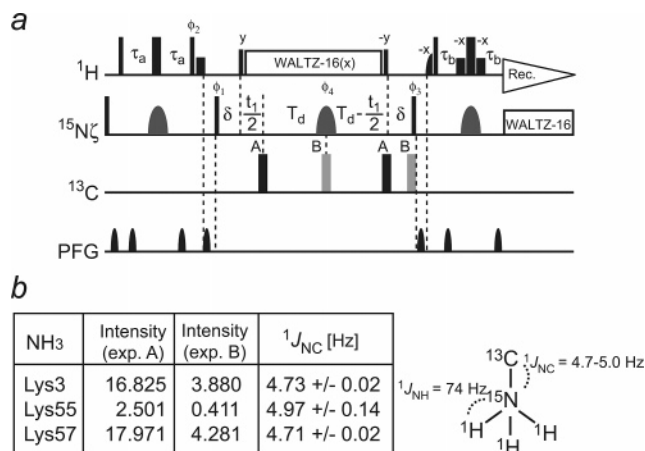


**Figure 9.** One bond  $^1J_{\text{NC}}$  scalar coupling between <sup>15</sup>N $\zeta$  and <sup>13</sup>C $\epsilon$  nuclei in Lys residues. (a) The spin-echo difference constant-time 2D <sup>1</sup>H–<sup>15</sup>N correlation experiment used for the measurement of  $^1J_{\text{NC}\zeta\epsilon}$  couplings. The delays  $\delta$  and  $T_d$  were set to 2.6 and 42.4 ms, respectively. Phase cycles:  $\phi_1 = \{x, -x\}$ ;  $\phi_2 = y$ ;  $\phi_3 = x$ ;  $\phi_4 = \{2x, 2y, 2(-x), 2(-y)\}$ ; rec. =  $\{x, -x, -x, x\}$ . Other experimental conditions are the same as those for Figure 4c. Two subexperiments A and B (with <sup>13</sup>C 180° pulses at the indicated positions) were carried out in an interleaved manner.  $^1J_{\text{NC}}$  can be calculated from  $I_B/I_A = \cos\{\pi^1J_{\text{NC}}(2\delta + 2T_d)\}$ , where  $I_A$  and  $I_B$  are peak intensities in subexperiments A and B, respectively. (b) Measured  $^1J_{\text{NC}}$  values for the NH<sub>3</sub> groups of Lys3, Lys55, and Lys57.

NH<sub>3</sub> group of Lys57, the values were  $18.7 \pm 0.3$  s<sup>-1</sup> at 35 °C and  $6.9 \pm 0.3$  s<sup>-1</sup> at 25 °C, which are only slightly smaller than the values of  $R_{\text{sc}}$  at the corresponding temperatures (cf. Table 1). Thus, we can conclude that water exchange constitutes the dominant contribution to  $R_2^{\text{in}}$  and  $R_2^{\text{out}}$  for <sup>15</sup>N transverse magnetization of NH<sub>3</sub> groups.

On the basis of the above experimental data, we can now explain why the HISQC experiment is far superior to the HSQC experiment with respect to the observation of <sup>1</sup>H–<sup>15</sup>N correlations for NH<sub>3</sub> groups (cf. Figure 5): specifically the dramatic difference between the two spectra can be directly attributed to the impact of rapid water exchange for NH<sub>3</sub> groups. In the case of the HISQC, <sup>15</sup>N transverse coherence is forced to be in-phase with respect to <sup>1</sup>H during the  $t_1$ (<sup>15</sup>N)-evolution period by the <sup>1</sup>H WALTZ-16 decoupling sequence. As long as the in-phase term is kept, there is no contribution from scalar relaxation to <sup>15</sup>N relaxation.<sup>7</sup> Thus, for the HISQC experiment, <sup>15</sup>N transverse relaxation during the  $t_1$ -evolution period is determined by the  $R_2^{\text{slow}}$  and  $R_2^{\text{fast}}$  rates rather than the  $R_2^{\text{in}}$  and  $R_2^{\text{out}}$  rates, and is therefore independent of water exchange. In the HSQC experiment, on the other hand, <sup>15</sup>N transverse coherence starts and ends as  $2N_yH_z$  and during the  $t_1$ -evolution period antiphase terms with respect to <sup>1</sup>H, such as  $4N_xH_zH_z$  and  $8N_yH_zH_zH_z$ , are present. Transverse relaxation in the <sup>15</sup>N-dimension of the HSQC is therefore characterized by the  $R_2^{\text{in}}$  and  $R_2^{\text{out}}$  rates, which are governed by rapid water-exchange for the NH<sub>3</sub> group. This effect results in significantly broader <sup>15</sup>N line shapes for the NH<sub>3</sub> cross-peaks in the HSQC spectrum. Indeed, the <sup>15</sup>N line shapes for the cross-peaks of the Lys3 and Lys55 NH<sub>3</sub> groups, both of which exhibit large  $k_{\text{ex}}^{\text{water}}$  exchange rates (Figure 7c), are broader in the HSQC spectrum (Figure 5b) and consequently the sensitivity improvement for these cross-peaks in the HISQC spectrum (Figure 5c) is even more dramatic than that for the

(38) Hwang, T. L.; Mori, S.; Shaka, A. J.; van Zijl, P. C. M. *J. Am. Chem. Soc.* **1997**, *119*, 6203–6204.

(39) Hwang, T. L.; van Zijl, P. C. M.; Mori, S. *J. Biomol. NMR* **1998**, *11*, 221–226.

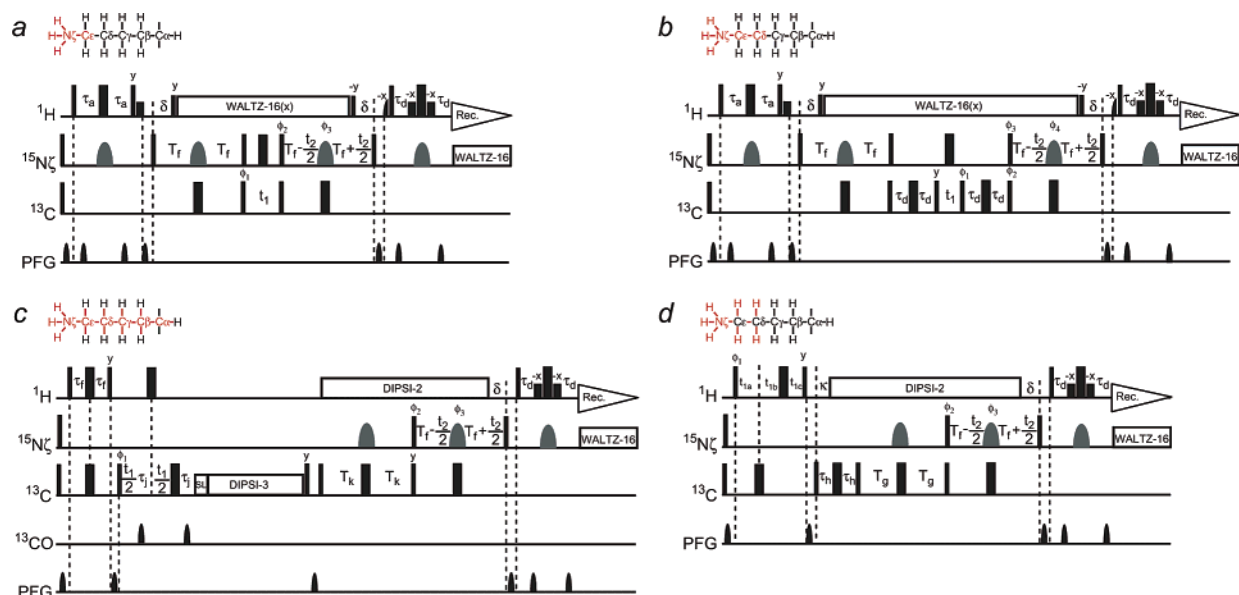


**Figure 10.** Suite of four 3D triple resonance experiments for the assignment of the  $^1\text{H}$  and  $^{15}\text{N}$  resonances of Lys  $\text{NH}_3$  groups: (a)  $\text{H}_3\text{NCE}$ , (b)  $\text{H}_3\text{NCECD}$ , (c)  $(\text{H})\text{CCENH}_3$ , and (d)  $\text{HDHE}(\text{CDCE})\text{NH}_3$ . Correlations observed along a lysine side chain for each experiment are indicated in red above the pulse sequences. Bars and shapes representing pulses are as defined in Figure 4.  $^1\text{H}$  composite pulses are applied with  $\gamma B_1/2\pi = 3.3$  kHz. Delays commonly used in these experiments are:  $\tau_a = 2.7$  ms;  $\delta = 2.6$  ms; and  $T_f = 45$  ms. Gradients were optimized to minimize the water signal. (a) 3D  $\text{H}_3\text{NCE}$  experiment. Hard  $^{13}\text{C}$  pulses are applied with  $\gamma B_1/2\pi = 17$  kHz. Phase cycles are  $\phi_1 = \{x, -x\}$ ;  $\phi_2 = \{2x, 2(-x)\}$ ;  $\phi_3 = x$ ; rec. =  $\{x, 2(-x), x\}$ . Phases for states-TPPI are  $\phi_1$  and  $\phi_2$  for the  $^{13}\text{C}$  and  $^{15}\text{N}$  dimensions, respectively. (b) 3D  $\text{H}_3\text{NCECD}$  experiment. The delay  $\tau_d$  was set to 3.3 ms to observe both  $^{13}\text{C}$  and  $^{13}\text{C}\delta$ . Phase cycles are  $\phi_1 = \{2y, 2(-y)\}$ ;  $\phi_2 = \{2x, 2(-x)\}$ ;  $\phi_3 = \{x, -x\}$ ;  $\phi_4 = \{4x, 4y\}$ ; rec. =  $\{x, 2(-x), x, -x, 2x, -x\}$ . Phases for states-TPPI are  $\phi_1$  and  $\phi_2$  for the  $^{13}\text{C}$  and  $^{15}\text{N}$  dimensions, respectively. (c) 3D  $(\text{H})\text{CCENH}_3$  experiment. A  $^{13}\text{C}$  DIPSI-3<sup>53</sup> pulse train along  $y$  was applied at 43 ppm with  $\gamma B_1/2\pi = 7.1$  kHz (mixing time, 23 ms). Prior to the DIPSI-3 pulse train, a  $^{13}\text{C}$  spin-lock (1 ms) is applied along  $x$ . Delays are  $\tau_f = 1.6$  ms;  $\tau_j = 1.1$  ms; and  $T_k = 14.3$  ms. Phase cycles are  $\phi_1 = \{x, -x\}$ ;  $\phi_2 = \{2x, 2(-x)\}$ ;  $\phi_3 = \{4x, 4y\}$ ; rec. =  $\{x, 2(-x), x, -x, 2x, -x\}$ . Phases for states-TPPI are  $\phi_1$  and  $\phi_2$  for the  $^{13}\text{C}$  and  $^{15}\text{N}$  dimensions, respectively. (d) 3D  $\text{HDHE}(\text{CDCE})\text{NH}_3$  experiment. Delays are  $\tau_h = 3.3$  ms;  $\kappa = 1.8$  ms; and  $T_g = 17.6$  ms. Acquisition for the indirect  $^1\text{H}$  dimension was achieved with a semiconstant time scheme<sup>26</sup> with  $t_{1a}$ ,  $t_{1b}$ , and  $t_{1c}$  satisfying the relationships  $(t_{1a} + t_{1b} - t_{1c}) = t_1$  and  $(t_{1a} - t_{1b} + t_{1c}) = 3.2$  ms. Phase cycles are  $\phi_1 = \{x, -x\}$ ;  $\phi_2 = \{2x, 2(-x)\}$ ;  $\phi_3 = \{4x, 4y\}$ ; rec. =  $\{x, 2(-x), x, -x, 2x, -x\}$ . Phases for states-TPPI are  $\phi_1$  and  $\phi_2$  for the  $^1\text{H}$  and  $^{15}\text{N}$  dimensions, respectively.

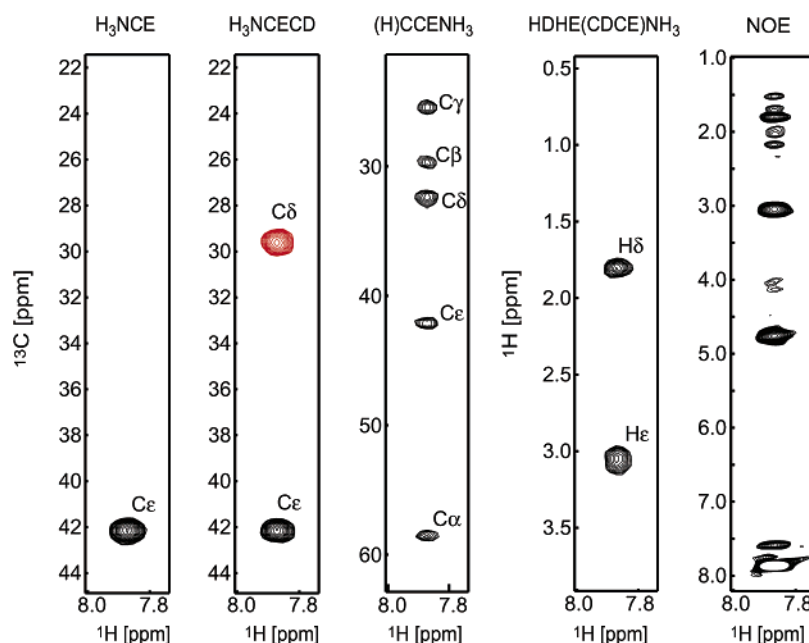


**Figure 11.** 2D slices taken from the four 3D  $\text{NH}_3$ -selective triple resonance experiments illustrating correlations observed for the  $\text{NH}_3$  group of Lys57. The pulse sequences for the triple resonance through-bond correlation experiments are those shown in Figure 10. The NOE spectrum was recorded using a 2D  $^1\text{H}$ – $^1\text{H}$  NOE experiment in which the NOE component is followed by a  $\text{NH}_3$ -selective HMQC scheme (using  $^{15}\text{N}$   $90^\circ$  E-BURP2 pulses to selectively excite the  $\text{NH}_3$  region) without  $^{15}\text{N}$  evolution. All spectra were recorded on the  $^{15}\text{N}/^{13}\text{C}$ -labeled HOXD9 homeodomain–DNA complex at  $25^\circ\text{C}$  at a  $^1\text{H}$  frequency of 500 MHz.

cross-peak of Lys57 which exhibits the slowest  $k_{\text{ex}}^{\text{water}}$  exchange rate.

To understand the  $^{15}\text{N}$  relaxation process in the HISQC experiment, we analyzed  $^{15}\text{N}$  transverse relaxation for the in-

phase single quantum term  $N_x$  using the pulse sequence shown Figure 8a. The relaxation rates, referred to as  $R_2^{\text{app}}(N_x)$ , were obtained from a single-exponential fit to the initial decay (Figure 8b,c). This analysis is only meaningful in a phenomenological sense, since theoretically the relaxation process should be biexponential and given by

$$I(T) = I(0)\{a_{\text{in}} \exp(-R_2^{\text{slow}}T) + a_{\text{out}} \exp(-R_2^{\text{fast}}T)\} \quad (8)$$

where  $a_{\text{in}}$  and  $a_{\text{out}}$  represent the populations of the inner and outer components at time zero. (Note that  $R_2^{\text{slow}}$  and  $R_2^{\text{fast}}$  rather than  $R_2^{\text{in}}$  and  $R_2^{\text{out}}$  are included because  $N_x$  is independent of scalar relaxation). In practice, accurate determination of rate constants using biexponential fitting is difficult as pointed out previously.<sup>30,31</sup> The apparent transverse relaxation rate from the initial slope is given by  $a_{\text{in}}R_2^{\text{slow}} + a_{\text{out}}R_2^{\text{fast}}$ . For the pulse sequence in Figure 8a, values of  $a_{\text{in}}$  and  $a_{\text{out}}$  should be close to 0.25 and 0.75, respectively, but will depend on the experimental conditions such as the delay  $\tau_b$ .<sup>30</sup> For Lys57 NH<sub>3</sub>, the value of  $0.25R_2^{\text{slow}} + 0.75R_2^{\text{fast}}$  is calculated to be  $3.8 \pm 0.32 \text{ s}^{-1}$  at 35 °C and  $3.3 \pm 0.09 \text{ s}^{-1}$  at 25 °C (Table 1). These values are reasonably close to those obtained for  $R_2^{\text{app}}(N_x)$ :  $4.45 \pm 0.15 \text{ s}^{-1}$  at 35 °C and  $4.41 \pm 0.10 \text{ s}^{-1}$  at 25 °C. Thus, <sup>15</sup>N transverse relaxation of the in-phase terms that are exclusively observed in the HISQC experiment is indeed independent of scalar relaxation owing to water exchange and, therefore, significantly slower.

**Triple Resonance NMR Experiments for Assignment of Lys NH<sub>3</sub>.** The <sup>1</sup>J-coupling between <sup>15</sup>Nζ and <sup>13</sup>Cε of lysine residues were measured using the spin-echo difference constant-time <sup>1</sup>H-<sup>15</sup>N HSQC experiment shown in Figure 9a. In this experiment, the <sup>1</sup>H-composite decoupling pulses applied after the delay δ maintain <sup>15</sup>N in-phase terms during the 2T<sub>d</sub> period, ensuring high sensitivity through the elimination of scalar relaxation during the <sup>15</sup>N-chemical shift evolution period. The measured <sup>1</sup>J<sub>CN</sub> values range from 4.7 to 5.0 Hz (Figure 9b) and are considerably smaller than the <sup>1</sup>J<sub>CαN</sub> coupling between backbone <sup>15</sup>N and <sup>13</sup>Cα (9–11 Hz).<sup>41</sup>

We designed a suite of triple resonance NMR experiments for through-bond correlations between <sup>15</sup>NH<sub>3</sub> and other <sup>1</sup>H and <sup>13</sup>C resonances within a lysine residue (Figure 10). The four pulse sequences termed H<sub>3</sub>NCE, H<sub>3</sub>NCECD, (H)CCENH<sub>3</sub>, HDHE(CDCE)NH<sub>3</sub> experiments (Figure 10, parts a, b, c, and d, respectively) are equivalent to HNCA,<sup>40</sup> HNCACB,<sup>42</sup> (H)CNH,<sup>43</sup> and HBHA(CBCA)NH<sub>3</sub><sup>44</sup> experiments, respectively, but optimized for NH<sub>3</sub> groups. Because of the <sup>15</sup>N relaxation properties of the NH<sub>3</sub> group described above, these experiments were designed to keep <sup>15</sup>N transverse magnetization in-phase with respect to <sup>1</sup>H as long as possible. While Grzesiek and Bax originally proposed a similar concept for experiments involving the backbone amide group,<sup>40</sup> it is critically important for NH<sub>3</sub>. Since the new experiments make use of a relatively small <sup>1</sup>J<sub>CN</sub> between <sup>15</sup>Nζ and <sup>13</sup>Cε (4.7–5.0 Hz), the coherence transfer requires a longer period for <sup>15</sup>N transverse magnetization than the corresponding experiments for backbone amide groups.

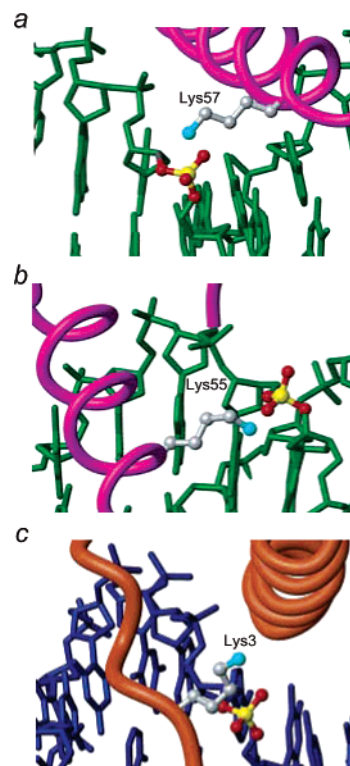


**Figure 12.** Location of the observed lysine NH<sub>3</sub> groups in the crystal structures of homeodomain–DNA complexes. Lysine residues and interacting DNA–phosphate groups are depicted as ball-and-sticks. All lysine NH<sub>3</sub> groups observed in the present study interact with a DNA phosphate group. Panels a and b show the interaction of Lys57 and Lys55, respectively, with a DNA–phosphate group seen in the crystal structure of the engrailed homeodomain–DNA complex (PDB accession code 3HDD).<sup>45</sup> These two lysine residues are conserved among the Q50-class homeodomains.<sup>45,46</sup> Panel c illustrates the interaction of Lys3 with a DNA–phosphate group seen in the crystal structure of the Msx-1 homeodomain–DNA complex (PDB entry 1IG7).<sup>47</sup> Lys3 is less well conserved than the other two lysine residues and is only observed in the crystal structure of the Msx-1 homeodomain–DNA complex. The intermolecular N⋯O distances between the NH<sub>3</sub> and DNA phosphate groups are 3.2 and 2.9 Å for Lys55 and Lys57, respectively, consistent with the presence of intermolecular hydrogen bonds or salt bridges. Although the distance between Lys3 NH<sub>3</sub> and a DNA phosphate group is 5.4 Å, a simple rotation about the χ<sub>3</sub> side-chain torsion angle can readily reduce this distance to less than 3.0 Å.

However, these experiments for NH<sub>3</sub> groups are intrinsically sensitive owing to very slow relaxation of in-phase <sup>15</sup>N transverse magnetization that satisfies the condition  $(2^1J_{\text{CN}})^{-1} < R_2(N_x)^{-1}$ . Figure 11 illustrates spectra recorded with these pulse sequences. Using the triple resonance data and lysine <sup>1</sup>H and <sup>13</sup>C resonances that had been assigned in a previous study,<sup>12</sup> we were able to assign the NH<sub>3</sub> signals seen in the HISQC spectrum to Lys3, Lys55, and Lys57 as shown in Figure 5c.

**Observed Lys NH<sub>3</sub> Groups Are Involved in Interaction with DNA.** The locations of the NH<sub>3</sub> groups of Lys3, Lys55, and Lys57 in the crystal structures of homeodomain–DNA complexes are shown in Figure 12. While the crystal structure of the HOXD9 homeodomain–DNA complex has not been determined, crystal structures of other homeodomain–DNA complexes that are highly homologous to the present system are available,<sup>45–47</sup> and our previous NMR studies have shown

(40) Grzesiek, S.; Bax, A. *J. Magn. Reson.* **1992**, *96*, 432–440.

(41) Delaglio, F.; Torchia, D. A.; Bax, A. *J. Biomol. NMR* **1991**, *1*, 439–446.

(42) Wittekind, M.; Mueller, L. *J. Magn. Reson., Ser. B* **1993**, *101*, 201–205.

(43) Logan, T. M.; Olejniczak, E. T.; Xu, R. X.; Fesik, S. W. *FEBS Lett.* **1992**, *314*, 413–418.

(44) Wang, A. C.; Lodi, P. J.; Qin, J.; Vuister, G. W.; Gronenborn, A. M.; Clore, G. M. *J. Magn. Reson., Ser. B* **1994**, *105*, 196–198.

(45) Fraenkel, E.; Rould, M. A.; Chambers, K. A.; Pabo, C. O. *J. Mol. Biol.* **1998**, *284*, 351–361.

(46) Fraenkel, E.; Pabo, C. O. *Nat. Struct. Biol.* **1998**, *5*, 692–697.

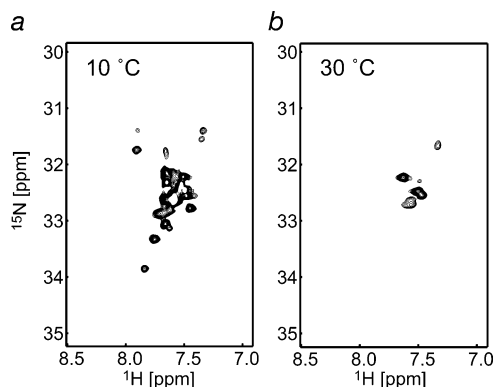


**Figure 13.**  $\text{NH}_3$ -selective HSQC spectra of the 128 kDa  $^{15}\text{N}$ -labeled enzyme I dimer ( $2 \times 579$  residues) from *Thermoanaerobacter tengcongensis* recorded at (a) 10 °C and (b) 30 °C. The NMR sample contained 0.4 mM enzyme I dissolved in 20 mM sodium acetate (pH 5.5), 0.1 mM  $\text{NaN}_3$ , and 2 mM DTT. Note that the sample is not deuterated. The experiments were recorded at 800 MHz using the pulse sequence shown in Figure 4c. Enzyme I contains 54 lysine residues, of which seven are involved in salt-bridge interactions with glutamate or aspartate residues in the crystal structures.<sup>50–52</sup> Cross-peaks observed at 30 °C are likely to arise from these  $\text{NH}_3$  groups owing to protection against rapid water exchange.

that the structure and mode of HOXD9 homeodomain binding to DNA is essentially the same.<sup>12</sup> In the crystal structures, the  $\text{NH}_3$  groups of Lys55 and Lys57 form hydrogen bonds with DNA phosphate groups ( $\text{N}\cdots\text{O}$  distances: 3.2 Å for Lys55; 2.9 Å for Lys57). Only the crystal structure of the Msx-1 homeodomain–DNA complex<sup>47</sup> contains coordinates of Lys3, and it is also close to a DNA phosphate group. These results indicate that lysine  $\text{NH}_3$  groups involved in hydrogen bonding/salt bridge interactions are easier to observe since they are partially protected from rapid water exchange. (Note, while water exchange does not affect in-phase  $^{15}\text{N}$  transverse relaxation it does cause significant line broadening in the  $^1\text{H}$  dimension). This unique feature allows for selective observation of  $\text{NH}_3$  groups involved in functional interactions, simply by adjusting pH and temperature.

**Potential Use of Lys  $\text{NH}_3$  as an Alternative Probe for Very Large Systems.** Recently Kay and co-workers have demonstrated that  $\text{CH}_3$  groups in an otherwise deuterated background are sensitive probes that can be analyzed for systems larger than 100 kDa.<sup>9,10,48</sup> For the same  $S_{\text{axis}}^2$  and  $\tau_r$ , relaxation of in-phase  $^{15}\text{N}$  transverse coherence for an  $\text{NH}_3$  group should be intrinsically slower than  $^{13}\text{C}$  relaxation for a  $\text{CH}_3$  group owing to the smaller nuclear gyromagnetic ratio of  $^{15}\text{N}$  relative to  $^{13}\text{C}$ . Thus, if water exchange is slow, lysine  $\text{NH}_3$  groups could potentially provide alternative probes for very large systems.

We tested this hypothesis using the 128 kDa dimer of  $^{15}\text{N}$ -labeled enzyme I at pH 5.5. HSQC spectra were measured at 10 and 30 °C (Figure 13). The water-exchange rates at 10 °C are expected to be  $\sim 9$ -fold slower than those at 30 °C.<sup>49</sup> Since

the value of the exchange rate at pH 5.5 and 10 °C is  $\sim 15 \text{ s}^{-1}$  for the  $\text{NH}_3$  group of a free lysine,<sup>4</sup> observation of many  $\text{NH}_3$  groups is feasible. Indeed, although the protein was not deuterated, many cross-peaks arising from  $\text{NH}_3$  groups of the 128 kDa enzyme I (54 lysine residues per monomer) were observed at 10 °C, of which  $\sim 10$  cross-peaks are isolated from the main cluster within the range of  $^{15}\text{N}$  chemical shifts between 31 and 34 ppm. At 30 °C, on the other hand, only  $\sim 6$  signals were observed because of the rapid water-exchange rates. The available crystal structures of enzyme I suggest that seven lysine residues make salt bridges with glutamate or aspartate carboxylate groups, with  $\text{N}\cdots\text{O}$  distances shorter than 3.2 Å.<sup>50–52</sup> The lysine  $\text{NH}_3$  signals observed at 30 °C are likely to arise from these residues.

**Concluding Remarks.** In this paper, we have described various aspects of heteronuclear  $^1\text{H}$ – $^{15}\text{N}$  NMR spectroscopy for lysine  $\text{NH}_3$  groups in proteins. In this study,  $^{15}\text{N}$  resonances for lysine  $\text{NH}_3$  groups were found to be located between 31 and 34 ppm. Even if the water-exchange rate is slow enough to permit observation of the proton  $\text{NH}_3$  resonances by 1D  $^1\text{H}$  NMR,  $^1\text{H}$ – $^{15}\text{N}$  cross-peaks arising from  $\text{NH}_3$  groups are rarely observed in a conventional HSQC experiment typically employed for backbone amide groups owing to the limited rf strength available for  $^{15}\text{N}$  pulses and severely broadened  $^{15}\text{N}$  line shapes. The  $^{15}\text{N}$  transverse relaxation properties of the  $\text{NH}_3$  group are unique in that they are highly affected by rapid water exchange via a mechanism that can be attributed to scalar relaxation of the second kind. As a consequence, neither HMQC nor HSQC experiments are optimal for the observation of  $\text{NH}_3$  correlations. In the latter experiments,  $^{15}\text{N}$  line shapes of the  $\text{NH}_3$  cross-peaks are even broader than those of backbone amide groups, although the intrinsic  $^{15}\text{N}$  relaxation rates of  $\text{NH}_3$  are much slower. The HSQC experiment presented here is not affected by scalar relaxation in the  $^{15}\text{N}$  dimension and therefore provides strikingly better resolution in the  $^{15}\text{N}$  dimension and much higher sensitivity for detection of  $\text{NH}_3$  correlations than either HSQC or HMQC experiments. Since  $^{15}\text{N}$  relaxation of in-phase terms is very slow, heteronuclear NMR experiments for Lys  $\text{NH}_3$  groups can be highly sensitive as long as the in-phase terms are maintained. Triple resonance experiments that implement this principle offer a useful means for assignment of lysine  $\text{NH}_3$  groups. Because of their favorable  $^{15}\text{N}$  relaxation properties, lysine  $\text{NH}_3$  groups offer alternative probes to methyl groups for studies involving systems in excess of 100 kDa, as demonstrated by the data obtained for the 128 kDa enzyme I dimer. For studies on protein–DNA complexes, the lysine  $\text{NH}_3$  cross-peaks observed at 35 °C are confined to those involved in direct interactions with DNA-phosphate groups. Indeed, because water exchange for  $\text{NH}_3$  groups involved in functional interactions (i.e., hydrogen bonds or salt bridges) tends to be slow (i.e., the protons are protected from exchange) such lysine  $\text{NH}_3$  groups are easier to characterize by heteronuclear NMR.

**Acknowledgment.** We thank Ad Bax and Dennis Torchia for useful discussions and Jun Hu for suggesting the use of a coaxial NMR tube. This work was supported by funds from the Intramural Program of the NIH and NIDDK and in part by the AIDS Targeted Antiviral program of the Office of the Director of the NIH (to G.M.C.).

JA0683436

(47) Hovde, S.; Abate-Shen, C.; Geiger, J. H. *Biochemistry* **2001**, *40*, 12013–12021.

(48) Sprangers, R.; Gribun, A.; Hwang, P. M.; Houry, W. A.; Kay, L. E. *Proc. Natl. Acad. Sci. U.S.A.* **2005**, *102*, 16678–16683.

(49) Englander, S. W.; Downer, N. W.; Teitelbaum, H. *Annu. Rev. Biochem.* **1972**, *41*, 903–924.

(50) Oberholzer, A. E.; Bumann, M.; Schneider, P.; Bachler, C.; Siebold, C.; Baumann, U.; Erni, B. *J. Mol. Biol.* **2005**, *346*, 521–532.

(51) Marquez, J.; Reinelt, S.; Koch, B.; Engelmann, R.; Hengstenberg, W.; Scheffzek, K. *J. Biol. Chem.* **2006**, *281*, 32508–32513.

(52) Teplyakov, A.; Lim, K.; Zhu, P. P.; Kapadia, G.; Chen, C. C.; Schwartz, J.; Howard, A.; Reddy, P. T.; Peterkofsky, A.; Herzberg, O. *Proc. Natl. Acad. Sci. U.S.A.* **2006**, *103*, 16218–16223.

(53) Shaka, A. J.; Lee, C. J.; Pine, A. *J. Magn. Reson.* **1988**, *77*, 274–293.